Ni/Fe electrodes prepared by electrodeposition method over different substrates for oxygen evolution reaction in alkaline medium.

F. J. Pérez-Alonso, C. Adán*, S. Rojas, M. A. Peña, J. L. G. Fierro.

Instituto de Catálisis y Petroleoquímica (CSIC), C/Marie Curie 2, 28049, Madrid, Spain.

Abstract

A series of Ni/Fe electrodes have been prepared by electrodeposition of metal salt pre- cursors on different substrates. The surface morphology, chemical composition and elec- trochemical characteristics of these electrodes were studied by various physico-chemical techniques such as X-ray Photoelectron Spectroscopy (XPS) and Scanning Electron Micro- scopy (SEM). The electrochemical properties of the electrodes were examined by steady- state polarization curves. First, the influence of features such as Ni/Fe composition and type of substrate for the oxygen evolution reaction (OER) were determined by electro- chemical techniques in a conventional 3-electrodes cell. The overpotential for the OER is lower for the electrodes with the higher concentrations of Ni. The electrodes with a Ni/Fe composition of 75/25 wt.% electrodeposited on steel mesh and/or 75/25 and 50/50 wt.% on nickel foam result in the most active configurations for the OER. These electrodes were further tested as anodes for alkaline water electrolysis during at least 70 h. In order to understand their activity and stability, the used electrodes were also characterized by SEM and compared to the fresh electrodes. Among the compositions and substrates examined, the Ni50Fe50-Nf electrode exhibited the lowest overpotential (2.1 V) for the OER and the higher stability as anode in an alkaline water electrolysis cell.

Keywords: Electrodeposition method, Ni/Fe electrodes, Type of substrate, Alkaline water electrolysis, Durability test, Electrolyzer prototype

* Corresponding author. Universidad Rey Juan Carlos, C/ Tulipa´n s/n, 28933 Móstoles, Spain. Tel.: 34 914888095; fax: 34 914887068. E-mail addresses: cristina.adan@urjc.es, cristina_adandelgado@yahoo.es (C. Adán).

1. Introduction

Water electrolysis has been used during many years to obtaining C-decoupled H2. Although the current production of H2 from H2O electrolysis accounts to a mere ca. 1% of total H2 production, it is foreseen that this process could become a pivotal process in the sustainable energy scenario by producing large amounts of C-decoupled renewable H2 [1,2]. Recently, the use of renewable energy sources coupled to electrolyzers for the electrolysis of water is attracting a great deal of interest and it is in fact considered amongst the preferred options for storing renewable electricity into chemical energy as hydrogen [2e5]. In this scenario, wind energy is the more viable option to be used for the production of H2. This is because a significant fraction of the energy produced by wind turbines is generated during low demand periods. By using the excess of energy produced by wind tur- bines large amounts of renewable hydrogen can be produced from water electrolysis. H2 can be stored or used to supply fuel cell coupled to electrolyzers. However, the designing of more efficient and durable, cheaper, more active and robust cathode and anode electrodes, is imperative for the wider implementation of such technologies.

Alkaline water electrolysis comprises two reactions: hydrogen evolution reaction (HER) which takes place at the cathode, and oxygen evolution reaction (OER) which occurs at the anode electrode (Eqs. (1) and (2), respectively).

$$2H_2O + 2e^- \rightarrow H_2 + 2OH^- \qquad \text{(Eqn. 1)}$$

$$2OH^- \rightarrow \tfrac{1}{2}\, O_2 + H_2O + 2e^- \qquad \text{(Eqn. 2)}$$

It is desirable that those reactions would take place at lowest possible overpotentials in order to increase the effi- ciency of the electrolysis cell. The overvoltage of the OER has been identified as the greatest source of energy loss in water electrolysis. This can be realized by designing more efficient electrodes. In addition, during electrolysis operation, the anode can suffer corrosion processes resulting in higher overpotentials [6]. This overpotential is directly related to the potential difference necessary to drive the system at a given current density and therefore it has a tremendous impact in the cost of the hydrogen production [7].

It is recognized that nickel is amongst the most suitable active metals for alkaline electrolyzers [8], since it is highly chemically stable, relatively cheap and can operate as

cata- lytic substrate for both the anodic and cathodic reactions [8-10]. Its performance can be enhanced greatly when pre- pared as thin films by powder coating [11] even though, in this case, the adhesion of nickel powder onto the conductive support becomes a very difficult task. Various methods, with different degrees of success, have been used for this matter. One of the most used methods for the deposition of metal oxides over metallic subtracts is electrodeposition [7,12-14]. In this method, the cations of a salt are electrochemically reduced to its metal state onto a metallic substrate. First, a process involving the orientation of atoms takes place onto the surface of the desired subtract. Then, a process usually known as electrocrystallization takes place leading to the incorporation of the desired atoms at the electrode. The latter process is usually slower on metal electrodes, which makes the overall electrodeposition rate to be limited by this latter step. Sometimes the precipitation reactions take place on the surface of the electrodes (electrode-solution interface) as a result of electronic exchange that causes the change in the oxidation state of one of the present species.

Recent works have shown the advantage of using Ni-based
alloys with transition metals due to the high adsorption ability of Ni atoms and also to the fact that the introduction of a transition metal alters significantly the electronic properties of the system. Several transition metals such as Mo, Cu, Fe, V and Pt have been studied [13,15-18]. In particular, it has been reported that the incorporation of Fe improves significantly the electrocatalytic activity of Ni for the OER [13,19].

In this paper we report the performance towards the OER of a series of Ni/Fe electrodes with different composition pre- pared by electrodeposition of the metal precursors on different substrates. In addition, the stability of the electrodes has been tested in a laboratory electrolyzer prototype for 70 h under continuous operation.

2. Experimental procedure

2.1 Electrodeposition method

For the electrodeposition, a source solution containing the metal cations to be incorporated into the metal substrates was prepared. A series of electrocatalysts with Ni/Fe ratios of 25/ 75 wt.%, 50/50 wt.% and 75/25 wt.% were prepared onto the different substrates. The salt precursors were aqueous solu- tions of $NiSO_4 \cdot 6H_2O$ and $FeSO_4 \cdot 7H_2O$ with a total concentration of 0.018 M and the appropriate metal loading

to obtaining the desired Ni/Fe loadings shown above. A 0.025 M solution of ammonium sulfate was added to the electrolyte solution in order to stabilize and increase its conductivity. The pH of the electrolyte was adjusted to 3 in all the syntheses with H2SO4.

The electrodeposition processes were carried out by applying a constant cathodic current of 300 mA cm—2 during 30 s at 25 ◦C in a conventional three-electrode electrochemical glass cell using an Ag/AgCl electrode and 9.4 cm2 geometric area Pt wire as the reference and counter electrodes, respectively. The Ni/Fe electrodes were electrodeposited on four different sub- strates: nickel foam (Nf), stainless steel mesh (Sm), nickel mesh (Nm) and nickel sheet (Ns) all of them supplied by GoodFellow Company. The electrodes used for the physico- chemical and electrochemical characterization have a geometric surface area of 1 × 1 cm [2] (exposed apparent surface area of 2 cm [2]) and the more active electrodes were prepared on substrates with geometric area of 2 × 2 cm [2] to be tested in electrolyzer prototype. In all cases the ratio between the volume of the source solution and the electrode area was set at 50 mL of source solution for every 2 cm [2] of electrode geometric area.

2.1 *Physicochemical and electrochemical characterization*

The morphology and chemical composition of the Ni/Fe electrodes were examined using a Hitachi S-3000N scanning electron microscope, equipped with an energy-dispersive X- ray spectroscopy (EDS), Oxford Instruments INCAx-sight system. Samples were measured without prior preparation. For the EDS studies, at least five representative areas of each electrode were scanned; the electrode composition reported in this manuscript is an average of these EDS measurements. The analysis of the surface composition and chemical state of the electrodes was accomplished by X-ray photoelectron spectroscopy (XPS). XPS spectra were obtained with a VG Escalab 200R spectrometer equipped with MgKa ¼ 1253.6 eV X- ray source and a hemispherical electron analyzer working at abpass energy of 20 eV. The binding energies (BE) were referenced to the C 1s peak at 284.6 eV used as an internal standard to take into account charging effects.

A conventional three-electrode glass cell was used for electrochemical measurements at 25 ◦C. Mercury/mercurous oxide (Hg/HgO) electrode and a platinum sheet were used as the reference and the counter electrode, respectively. The evaluation of the performance

of the electrodes for the OER was conducted in an Ar-saturated 30 wt.% KOH electrolyte solution combining cyclic voltammetry analysis with steady- state polarization curves. Before the electrochemical tests, the working electrode was subjected to a program of 20 consecutive cyclic voltammetry scans from 0.9 to 1.6 V at20 mV s—1 in order to clean and activate the electrodes so that reproducible voltammograms were recorded at room temperature. Then, the performance of the electrodes for the OER was studied by obtaining potential current curves. The kinetics of the electrodes was obtained from the Tafel equation (a limiting case of the ButlereVolmer equation) which relates the recorded current density with the overpotential in the high overpotential region. Steady-state polarization curves were obtained at low scan rate of 0.5 mV s—1 between open circuit potential and 1.6 V vs. NHE.

2.3 Water alkaline electrolysis durability tests

The performance of selected electrodes for the OER was further tested in a laboratory electrolyzer prototype equipped with a 2 L tank of a 30 wt.% KOH electrolyte operating at 80 ◦C. The OER activity was studied by chronopotentiometry methods by applying a fixed current density of 300 mA cm—2 during 70 h. The electrolyzer consists of a Teflon (PTFE) elec- trolysis cell with three ports (see Fig. 1). Two of such ports are for electrolyte feed and vent and the third port is for placing the thermocouple. The electrolyte solution is driven contin- uously through the cell and to the glass tank by a peristaltic pump. The PTFE cell is connected to a PC controlled poten- tiostat/galvanostat through stainless steel metal connections. Selected data are collected during the whole experiment with a computer. Metal connections are in contact with the metallic anode and cathode electrodes. The electrodes used for these experiments have a geometric surface area of 2 × 2 cm [2]. In all the experiments the electrodes were tested as anodes for water electrolysis using a nickel foam plate as the cathode electrode.

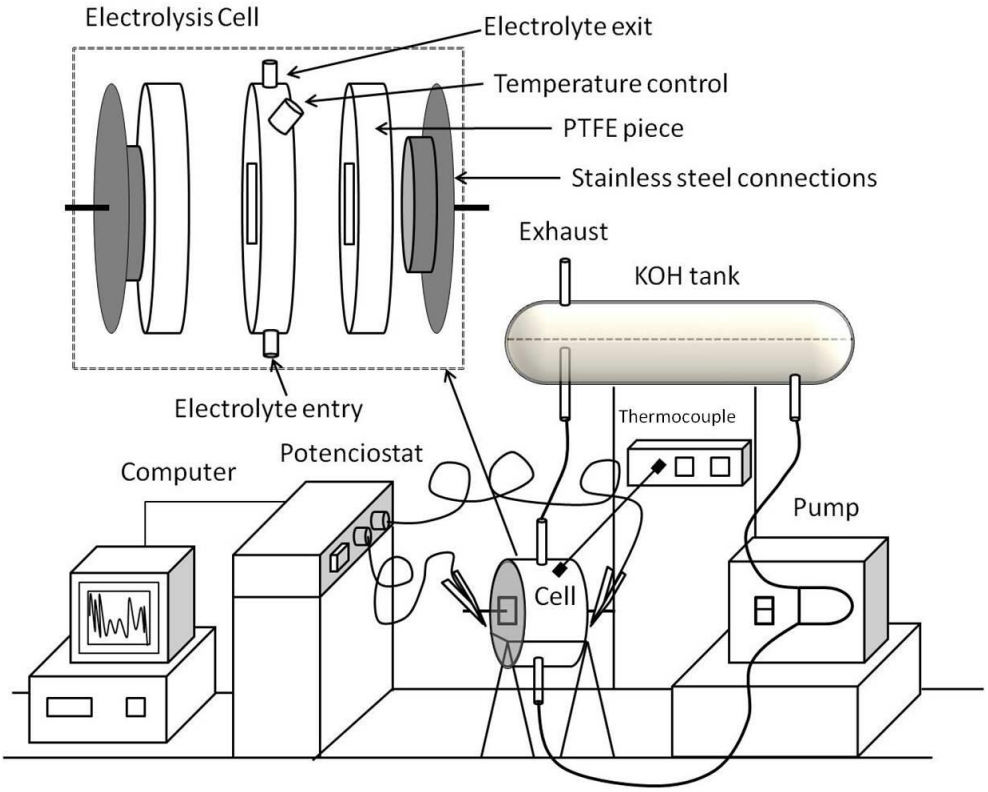

Figure 1. Experimental electrolyzer and electrolysis cell design.

3. Results and discussion

3.1. Ni/Fe composition and type of support

Eight electrodes were prepared with different Ni/Fe wt.% compositions over four types of substrates. Table 1 collects the nomenclature and the actual composition (derived from the EDS analyses) of the metallic phases in each of those electrodes. In all cases, the weight percent of Ni and Fe (metallic base) in the electrode is very close to the theoretical composition. However, this observation does not apply for the electrodes prepared with the Ni foam, (-Nf series). As observed in Table 1, the amount of Ni recorded with EDS is much higher than the expected value, especially in the Ni25Fe75-Nf elec- trode. This observation could be explained by assuming that the thickness of these electrodeposited electrodes is smaller than the penetration ability of the EDS probe which is able to reach the Ni-foam used as support, and as a consequence the amount of Ni is overestimated in the three electrodes.

Table 1. Electrodes alloy composition determined by EDS and thickness.

Electrocatalyst[a]	**Alloy composition in weight**		**Thickness (μm)**
	Ni (%)	**Fe (%)**	
Ni75Fe25-Nf	92.4±3.0	7.6±3.0	2.0±0.1
Ni50Fe50-Nf	--	--	--
Ni25Fe75-Nf	73.1±9.3	26.9±9.3	2.9±1.4
Ni75Fe25-Sm	70.1±7.5	29.9±7.5	3.8±0.3
Ni50Fe50-Sm	45.9±2.0	54.0±2.0	4.7±0.6
Ni25Fe75-Sm	26.2±2.3	73.8±2.3	3.6±0.2
Ni75Fe25-Ns	75.2±3.4	24.8±3.4	7.9±0.6
Ni75Fe25-Nm	77.1±3.5	22.9±3.5	4.5±0.7

[a]Electrocatalysts nomenclature (Nf: Nickel foam, Sm: Steel mesh, Ns: Nickel sheet, Nm: Nickel mesh).

Representative scanning electron microscopy images of the Ni/Fe electrodes deposited on the nickel foam are shown in Fig. 2. The images show a thin coated film distributed over the Ni foam. Only in some curved zones of the Ni foam several discontinuities of the Ni/Fe layer can be detected. More importantly, the distribution of foam supports is very similar for all samples, irrespectively of Ni/Fe loading. In all electrodes, the thickness of the Ni/Fe layers varies from 2.0 to 3.5 mm (see Table 1).

Fig. 3 shows selected SEM images of the Ni75Fe25 elec- trodes deposited on stainless steel mesh (Sm), nickel mesh (Nm) and nickel sheet (Ns). As shown in Fig. 3 the distribution of the Ni/Fe layer on the mesh-based substrates, stainless steel (upper panel in Fig. 3) and nickel mesh (lower panel in Fig. 3), is slightly different from that observed for the elec- trodes deposited on nickel foam (Fig. 2), showing a higher amount of discontinuities when the meshes are used. The Ni75Fe25-Ns electrode deposited on the nickel sheet displays a very different morphology than that of the other substrates, clearly showing the presence of a discontinuous flaky Ni/Fe layer with broken edges and with poor adherence to the sur- face of the Ni sheet.

The thicknesses of the Ni/Fe layers vary with the type of substrate employed, as shown in Table 1. Thus, the thickness of the Ni/Fe layer on the nickel foam substrate is of around 2e3 mm. Thicker Ni/Fe layers of around 4, 5 and 8 mm were formed on the

stainless steel and nickel mesh and the nickel sheet electrodes, respectively (see Table 1).

It should be recalled that even if all substrates have an apparent geometric surface area of 2 cm [2], their total area, considering the three-dimensional area due to the morphology of the electrode, is not the same in all the sub- strates employed. Thus, the nickel foam has a total area greater than the meshes and greater than the sheet because of the complexity of their morphology (see the morphology of the substrates in Figs. 2 and 3). Therefore, the different Ni/Fe layer thickness values shown in Table 1 clearly demonstrate that the total area of the substrates has a strong influence on the coating process, especially on the thickness of the cata- lytic layer of the electrodes prepared by electrodeposition methodology. Thus, when comparing the electrodes with the same Ni/Fe loadings, the substrate with the highest total area, i.e., the nickel foam, leads to the thinner Ni/Fe deposits in the series. On the other hand, the substrate with the smaller total area, the nickel sheet, exhibits the thicker layer in the series. The X-ray photoelectron spectra of the Fe 2p3/2 core-level region of the Ni/Fe electrodes deposited onto the nickel foam, the Nf series, are shown in Fig. 4a. As expected, the concentration of surface Fe increases with the Fe loading in the electrodes, as observed in Fig. 5 for Fe/Ni ratios obtained by XPS. Nevertheless, Fig. 5 shows that the surface Fe/Ni ratios are lower than the expected theoretical values. In this sense, the determination of the Fe/Ni ratio actually electrodeposited by XPS could be misleading since, as shown above, the Ni amount is overestimated because it probably includes a contribution of Ni of the foam support. As it has been indi- cated regarding the SEM pictures (Fig. 2), there are several discontinuities in the Fe/Ni layer on the curve zones. As a consequence, the Ni-foam support is accessible to the XPS analysis. On the other hand, and according to the Pourbaix diagrams, the reduction of Ni2þ cations and as a consequence their electrodeposition is more favored than the reduction-electrodeposition of Fe2þ under the reaction conditions (pH ¼ 3.0) chosen for the electrodeposition of the Fe/Ni layer.

This fact could also contribute to the observed Ni surface enrichment of electrodeposited layer. EDS analysis show a similar trend (low Fe/Ni values, Fig. 5), but in this case the differences are higher, since the depth spatial resolution is much lower than for XPS, so a greater contribution of the Ni- foam support is expected in the EDS analysis.

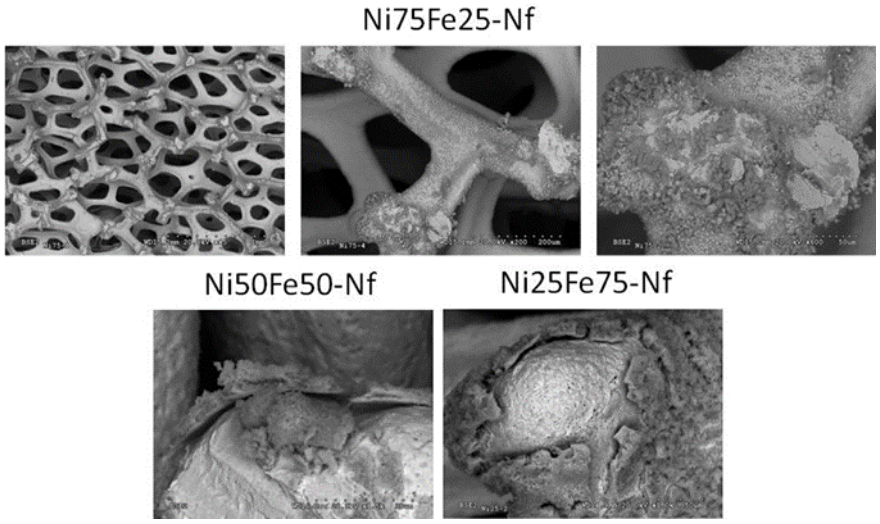

Fig. 2. SEM micrographs of the Ni/Fe electrodes deposited on the nickel foam (Nf).

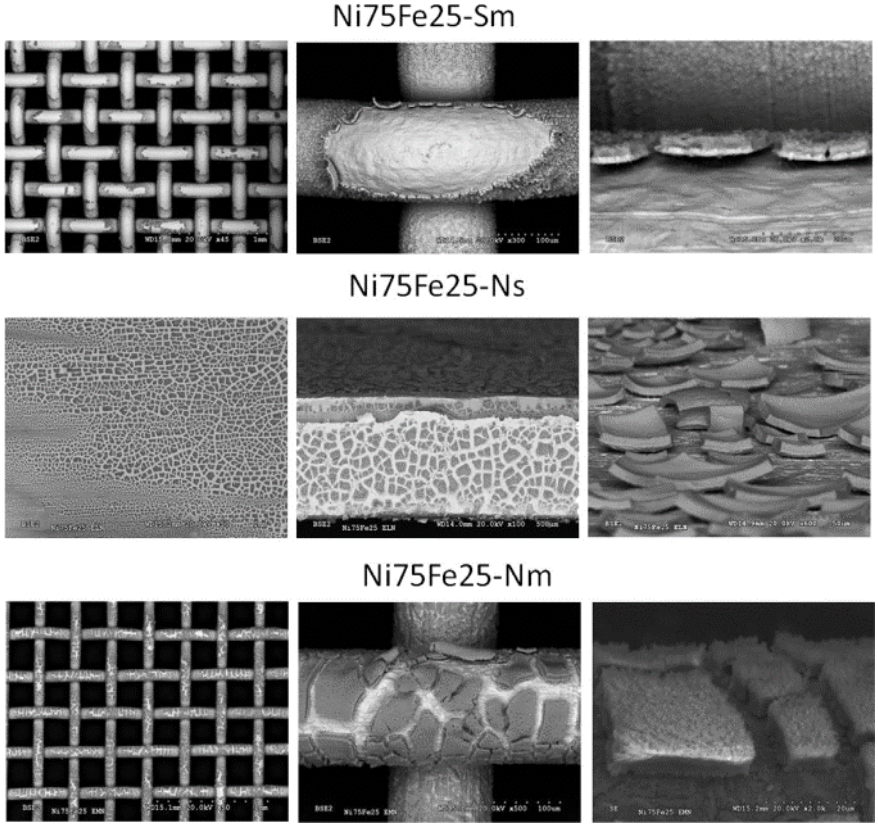

Fig. 3. SEM micrographs of the electrodes with a Ni/Fe ratio of 75/25 on different supports; stainless steel mesh (upper panel), nickel sheet (intermediate panel) and nickel mesh (lower panel).

Regarding the iron oxidation state, the binding energies of the Fe 2p3/2 peaks at 710.3 and 711.0 eV are assigned to Fe3þ, either as Fe2O3 or as hydroxide FeOOH species [19]. Similarly, the Ni 2p3/2 core-level spectra of all of the Nf electrodes are shown in Fig. 4b. The peaks at binding energy of ca. 855.3 eV are ascribed to Ni2þ species. The broad component at around and 859.5 eV and the less intense peak at around 864.6 eV are shake-up lines originated from Ni2þ ions in an environment of O2— ions [20]. It should be noted that the presence of reduced Ni is only observed by the appearance of a small peak at ca. 851 eV in the spectrum of Ni50Fe50-Nf.

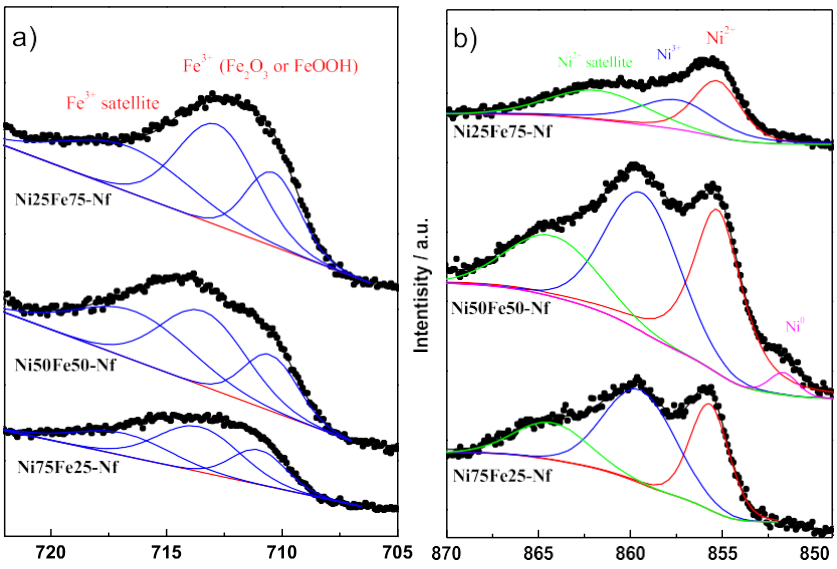

Fig. 4. (a) Fe 2p3/2 core-level spectra; (b) Ni 2p3/2 core-level spectra of the Ni/Fe electrocatalysts supported on nickel foam.

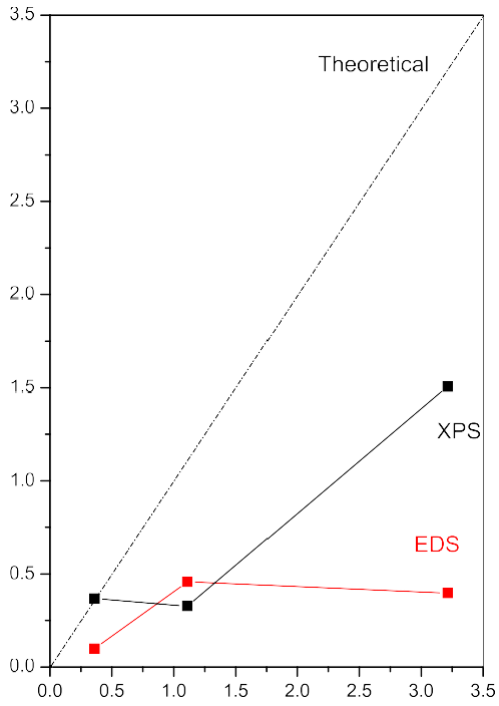

Fig. 5. Comparison of theoretical Fe/Ni atomic ratios and Fe/Ni atomic ratios determined by EDS and XPS of the Ni/Fe electrocatalysts supported on nickel foam.

The XPS results clearly show that the outer layer of the electrodeposited Ni/Fe layer is formed almost exclusively by oxidized phases of Fe and Ni. This observation suggests that the electrodeposited Ni/Fe layer is prone to be oxidized upon air exposure.

Fig. 6 shows the steady-state polarization curves recorded during the anodic sweep for the Ni/Fe electrodes deposited onto Ni foam (Fig. 6a) and stainless steel mesh (Fig. 6b). In general, the most significant differences between the perfor- mances of the electrodes are observed at low current den- sities. As the current density increases the electrodes overpotentials tend to reach similar values since at such high current densities the reaction are dominated by reactant diffusion process. However, the performance of the Ni/Fe- containing electrodes is clearly better than that of the bare substrates, especially for the Ni foam series. Irrespectively of the support, the overpotential for the OER decreases as the amount of Ni on the electrodeposited layer increases. Thus, the electrodes with a Ni/Fe ratio of 75/25 record lower over- potential values, especially when measured at low current densities. Fig. 7 shows the OER steady-state polarization curves recorded with the electrodes with the optimized Ni/Fe composition of 75/25 wt.% deposited onto the 4 substrates used in this work, nickel mesh, nickel sheet, nickel foam and stainless steel. Although as stated above, the composition of the

electrodeposited layer is the most important parameter which determines the OER activity, the nature of the substrate onto which the Ni/Fe layer is deposited also shows some in- fluence in the catalytic performance of the electrodes. Thus, the electrocatalysts prepared onto stainless steel mesh and nickel foam show better performances for the OER than those deposited onto the other supports. Two possibilities can be argued to explain this effect. On one hand, although all sup- ports samples have the same geometric surface area of 2 cm [2], the total area of the electrode changes with the morphology of the substrate, as it has been explained above. As a consequence, the real active area of the Ni/Fe electro- deposited layer should be the highest in the nickel foam se- ries. On the other hand, the support is active for the OER by itself, as observed in Fig. 6. Actually, steel mesh substrate shows considerably activity towards OER. This fact has been also observed previously by other authors [21].

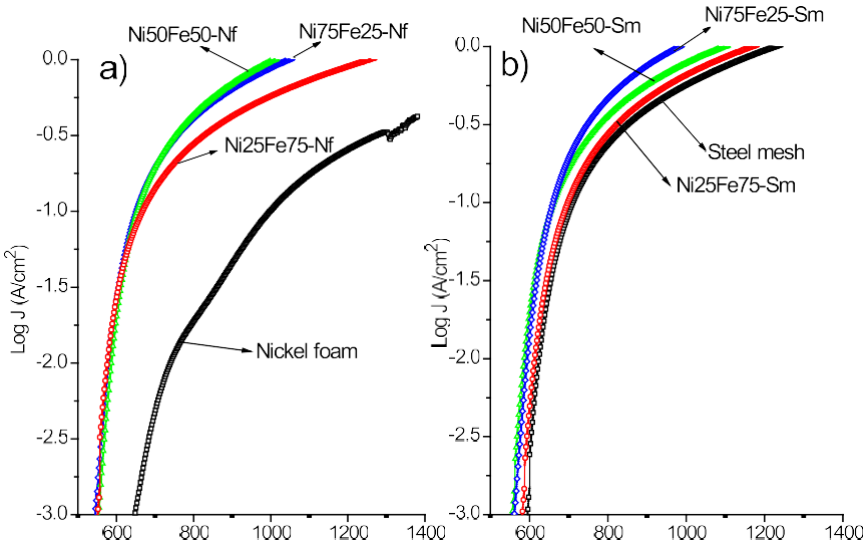

Fig. 6. Anodic steady-state polarization curves of the electrocatalysts at different Ni/Fe composition; (a) on nickel foam; (b) on steel mesh. Conditions: scan rate = $1mVs^{-1}$, KOH = 30 % wt.

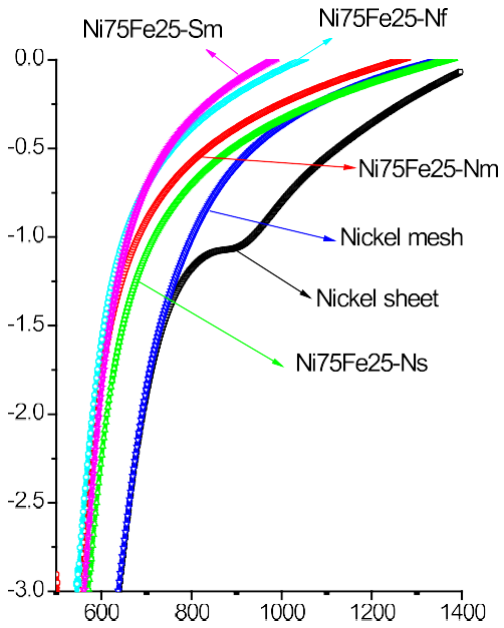

Fig. 7. Anodic steady-state polarization curves of the Ni75Fe25 electrocatalysts on different supports. Conditions: scan rate [1 mV sL1, KOH [30 wt.%. Conditions: scan rate = 1mVs^{-1}, KOH = 30 % wt.

Representative kinetic parameters for the OER have been extracted from Figs. 6 and 7. Tafel slope (b) and overpotential at two representative current densities of 100 (j100) and 300 (j300) mA cm—2 obtained dividing current per apparent unit geometric surface area are shown in Table 2. The Tafel slopes have been obtained by linear least square fitting of the linear part of the semi-logarithmic steady-state Tafel plots at over-potentials higher than 200 mV with respect the thermodynamic potential value of OER. In general, the Ni/Fe-modified electrodes show Tafel slopes of around 40 mV dec—1 whereas the bare substrates exhibit Tafel slopes of around 60 mV dec—1. It is well admitted that a Tafel slope of 40 mV dec—1 indicates that the rate-determining step of the OER reaction is a second electron transfer step from the hydroxylated active site to form the oxide: SeOH þ OH— ¼ SeO þ H2O þ e—, where “S” indicates the active site [22,23]. On the other hand, a slope of 60 mV dec—1 indicates that the rate-determining step is a chemical evolution of the unstable SeOH* to form more stable SeOH. The modi- fication of the Tafel slope after the deposition of the Ni/Fe layer onto the substrates leads to the modification of the na- ture of the active sites and as a consequence of the rate- determining step of the OER resulting in a more active electrocatalyst.

Table 2. Tafel parameters for OER on electrodeposited Ni/Fe electrodes in 30 wt.% KOH electrolyte.

Electrocatalyst	b (mV/dec)	j_{100} (mV)	j_{300} (mV)
Nickel foam	93	653	909
Ni75Fe25-Nf	40	306	406
Ni50Fe50-Nf	41	309	401
Ni25Fe75-Nf	38	322	471
Stain steel mesh	46	366	495
Ni75Fe25-Sm	40	315	396
Ni50Fe50-Sm	35	317	425
Ni25Fe75-Sm	35	353	469
Nickel sheet	57	590	768
Ni75Fe25-Ns	45	372	534
Nickel mesh	67	456	582
Ni75Fe25-Nm	45	337	480

As already mentioned, the bare substrates show moderate activities for the OER, lower than that of the Ni/Fe-modified electrodes. Both Ni/Fe-Nf and Ni/Fe-Sm series record the lower overpotential values at j100. On the other hand, the electrodes prepared on nickel sheet (-Ns series) show the higher overpotential in the series. These results are in line with previous reported data for OER in alkaline media using passivated polycrystalline nickel and Ni/Fe based electro- catalysts [24,25]. Lyons et al. studied OER performance of anodic passivated oxides of iron, cobalt and nickel. The overpotential reported for passivated polycrystalline nickel at 100 mA cm—2 was of around 540 mV which is very similar to the value reported here for nickel sheet [24]. On the other hand, Hu et al. studied the OER performance of Ni/Fe layers deposited over Cu plates in alkaline media. In this case, the overpotential values were around 400-425 mV at 100 mA cm—2 for Ni/Febased samples what are higher that values obtained for our Ni/Fe based electrodes prepared over nickel foam and stainless steel mesh [25]. Thus, the use of electrodeposition method to deposit Ni/Fe layers on nickel foam and stainless steel sub- strates appear to improve the OER activity.

The Ni/Fe based electrocatalysts showed the same trend when operating at higher current densities. Thus, the over- potential values recorded at 300 mA cm—2 for Ni75Fe25-Nf, Ni50Fe50-Nf and Ni75Fe25-Sm are the best in the series reaching values of 406, 401 and 396 mV, respectively. These overpotential values are 50 mV lower than

obtained by Hu et al. in previous reports with Ni/Fe based electrocatalysts [25] displaying again the improvement obtained when these types of substrates with a porous morphology are used.

It should be taken into account that the overpotential measured at 300 mA cm—2 lies within the potential region where the reaction may be controlled by diffusion of reactants. Furthermore, at high current values features such as bubble formation and removal from the electrode could play an important role in the overall OER process. The composition of the electrode is not the single relevant feature to define its catalytic performance; in fact, when working at such high current densities the morphology of the electrodes is expected to be a dominant factor for the OER activity for instance by allowing a facile removal of oxygen from the surface of the electrodes. The electrodes prepared on nickel foam and stainless steel mesh display the best OER performances at high current densities and as a consequence were chosen for further characterization in the electrolyzer prototype

3.2. Durability Test

It should be taken into account that the overpotential measured at 300 mA cm—2 lies within the potential region where the reaction may be controlled by diffusion of reactants. Furthermore, at high current values features such as bubble formation and removal from the electrode could play an important role in the overall OER process. The composition of the electrode is not the single relevant feature to define its catalytic performance; in fact, when working at such high current densities the morphology of the electrodes is expected to be a dominant factor for the OER activity for instance by allowing a facile removal of oxygen from the surface of the electrodes. The electrodes prepared on nickel foam and stainless steel mesh display the best OER performances at high current densities and as a consequence were chosen for further characterization in the electrolyzer prototype300 mV which means that a higher energy input is required for the Ni75Fe50-Sm electrode to keep the reaction running at the same rate than with Ni50Fe50-Nf. The initial efficiency of the electrolyzers, measured as the voltage efficiency [26] is of 67% for both electrodes; however, it decreases to 59% for the electrolyzer with Ni75Fe25-Sm. In this figure has been also included the potential obtained with an electrode of nickel foam. The average potential obtained with this electrode is of ca. 2.7 V; this value is significantly higher than that recorded for the

other two electrodes selected for this study. Further- more, the oscillation of the measurement is more evident which implies a different behavior of the electrodes prepared by the electrodeposition method. Fig. 9 shows selected SEM images of Ni75Fe25-Sm recorded after the stability experi- ments shown above. The images clearly show that the Ni/Fe layer has been almost completely detached off the substrate during the test in the electrolyzer. This observation could justify the observed higher overpotential of this electrode at the end of the experiment.

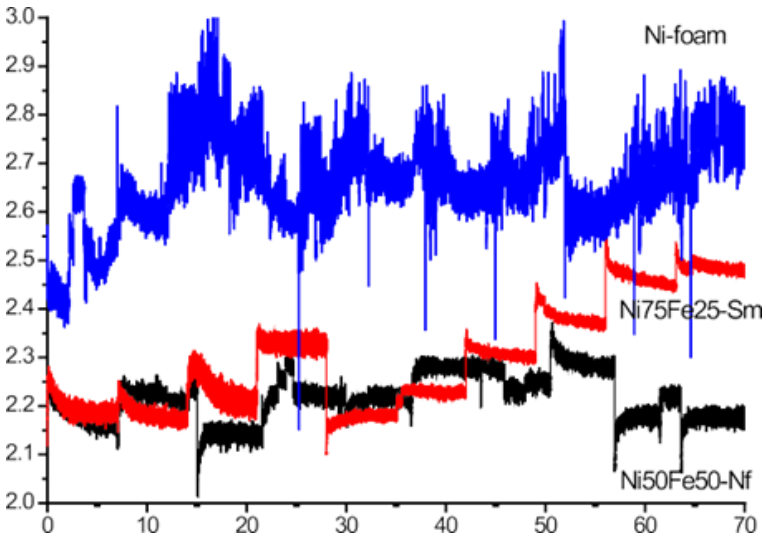

Fig. 8. Durability tests of Ni-foam, Ni50Fe50-Nf and Ni75Fe25-Sm electrodes measured during 70 h operation at j 300 mA cmL2 and 80 ◦C in 30 wt.% KOH.

Similarly, the SEM images of Ni50Fe50-Nf after the 70 h durability test show that the electrodeposited layer has been partially detached off of the electrode. In addition the elec- trodeposited layer has shrunk during operation and the thickness diminished from around 3 mme1 mm. Despite the loss of part of electrodeposited layer, this electrode keeps a stable potential operation for water electrolysis. These results could indicate that an important and enough part of Ni/Fe layer stays over the substrate to maintain the same level of activity. Thus, Nickel foam substrate apparently comprises better properties in terms of stability that steel mesh albeit more experiments are necessary to understand this phenomena.

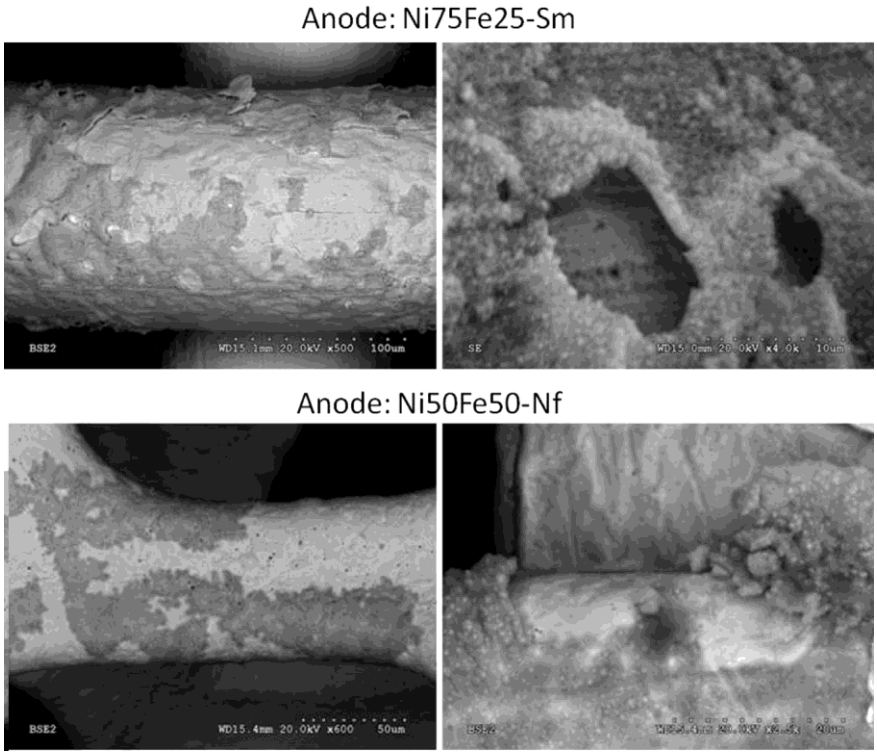

Fig. 9. SEM images of Ni50Fe50-Nf and Ni75Fe25-Sm electrodes recovered after the durability tests reported in Fig. 7.

In summary, Ni50Fe50-Nf shows the highest activity and more importantly stable overpotential of the series for the OER in 30 wt.% KOH solution at 80 ◦C during 70 h.

Conclusions

This work clearly shows that the activity of Ni/Fe anode electrodes for the OER varies with the Ni/Fe composition of each electrode and with the morphology of the substrate onto which they are deposited. Incorporation of iron as Fe2O3 or hydroxide species to the electrode has modified significantly the electronic properties of the system improving OER activ- ity. Nickel foam and steel mesh show the best properties as substrates. Electrocatalysts based on this substrates display the more homogeneous coating and lower thickness. Two electrodes have been selected with an optimum Ni/Fe ratio composition of 50/50 wt.% on nickel foam and 75/25 wt.% on steel mesh substrates for their lower overpotential in the OER. Moreover, durability tests have demonstrated that Ni50Fe50- Nf electrode has the optimum configuration to work as anode, providing stable overpotential at 2.2 V in an alkaline electrolyzer.

Acknoweledgements

ACCIONA Energía and Ingeteam are acknowledged for allow- ing publication of these results obtained in the framework of CENIT-SPHERA project. Project ENE2010-15381 from the Spanish Education and Science Ministry is also acknowledged.
C. Adán thanks the MICINN for the Juan de la Cierva post- doctoral contract (JCI-2010-06430).

References

[1] LeRoy RL, Stuart AK. In: Srinivasan S, Salzano FJ, Landgrebe AR, editors. Industrial water electrolysis. Princeton: The Electrochemical Society; 1978. p. 117.
[2] Orecchini F, Santiangeli A, Dell'Era A. A technological solution for everywhere energy supply with sun, hydrogen and fuel cells. J Fuel Cell Sci Technol 2006;3(1):75e82.
[3] Rzayeva MP, Salamov OM, Kerimov MK. Modelling to get hydrogen and oxygen by solar water electrolysis. Int J Hydrogen Energy 2001;26:195-201.
[4] Marcelo D, Dell'Era A. Economical electrolyser solution. Int J Hydrogen Energy 2008;33:3041-4.
[5] Barbir F. Transition to renewable energy systems with hydrogen as an energy carrier. Energy 2009;34:308-12.
[6] Bocca C, Barbucci A, Delucchi M, Cerisola G. Nickelecobalt oxide-coated electrodes: influence of the preparation technique on oxygen evolution reaction (OER) in an alkaline solution. Int J Hydrogen Energy 1999;24:21-6.
[7] Gonza´lez ER, Avaca LA, Carubelli A, Tanaka AA, Tremiliosi- Filho G. The hydrogen evolution reaction on mild steel and nickeleiron codeposits in alkaline media. Int J Hydrogen Energy 1984;9:689-93.
[8] Lu G, Zangari G. Study of the electroless deposition process of Ni-p-based ternary alloys. J Electrochem Soc 2003;150:777-86.
[9] Divisek J, Malinowski P, Nergel J, Schmitz H. Improved components for advanced alkaline water electrolysis. Int J Hydrogen Energy 1988;13:141-50.

[10] Miles MH, Kissel G, Lu PWT, Srinivasan S. Effect of temperature on electrode kinetic parameters for hydrogen and oxygen evolution reactions on nickel electrodes in alkaline solutions. J Electrochem Soc 1976;123:332-6.

[11] Boccaccini AR, Roether JA, Thomas BJC, Shaffer MSP, Chavez E, Stoll E, et al. The electrophoretic deposition of inorganic nanoscaled materials. J Ceram Soc Jpn 2006;114(1):1-14.

[12] De Carvalho J, Tremiliosi-Filho G, Avaca LA, Gonzalez ER. Electrodeposits of iron and nickeleiron for hydrogen evolution in alkaline solutions. Int J Hydrogen Energy 1989;14(3):161e5.

[13] Plata-Torres M, Torres-Huerta AM, Dominguez-Crespo MA, Arce-Estrada EM, Ramirez-Rodrı´guez C. Electrochemical performance of crystalline NieCoeMoeFe electrodes obtained by mechanical alloying on the oxygen evolution reaction. Int J Hydrogen Energy 2007;32:4142-52.

[14] Orina´cova´ R, Turonova´ A, Kladekova´ D, Ga´lova´ M, Smith RM. Recent developments in the electrodeposition of nickel and some nickel-based alloys. J Appl Electrochem 2006;36:957-72.

[15] Kawashima A, Sakaki T, Habazaki H, Hashimoto K. NieMoeO alloy cathodes for hydrogen evolution in hot concentrated NaOH solution. Mater Sci Eng A 1999;267:246-53.

[16] Raj IA, Vasu KI. Transition metal-based hydrogen electrodes in alkaline solution e electrocatalysis on nickel based binary alloy coatings. J Appl Electrochem 1990;20:32-8.

[17] Kaninski MPM, Nikolic VM, Tasic GS, Rakocevic ZLj. Electrocatalytic activation of Ni electrode for hydrogen production by electrodeposition of Co and V species. Int J Hydrogen Energy 2009;34:703-9.

[18] Panek J, Budniok A. Production and electrochemical characterization of Ni-based composite coatings containing titanium, vanadium or molybdenum powders. Surf Coat Technol 2007;201:6478-83.

[19] Merrill MD, Dougherty RC. Metal oxide catalysts for the evolution of O2 from H2O. J Phys Chem C 2008;112:3655-66.

[20] Wagner CD, Riggs WM, Davis LE, Moulder JF. In: Muilenberg GE, editor. Handbook of X-ray photoelectron spectroscopy. Perkin-Elmer Corporation (Physical Electronics); 1979.

[21] Fricoteaux P, Rousse C. Influence of substrate, pH and magnetic field onto composition and current efficiency of electrodeposited NieFe alloys. J Electroanal Chem 2008;612:9-14.

[22] Guerini E, Piozzini M, Castelli A, Colombo A, Trassatti S. Effect of FeOx on the electrocatalytic properties of NiCo2O4 for O2 evolution from alkaline solutions. J Solid State Electrochem 2008;12:363-73.

[23] Trassatti S. Electrode kinetics and electrocatalysis of hydrogen and oxygen electrode reactions. In: Wendt H, editor. The oxygen evolution reaction, 4. Amsterdam: Electrochemical hydrogen technologies Elsevier; 1990. p. 104-35.

[24] Lyons MEG, Brandon MP. A comparative study of the oxygen evolution reaction on oxidised nickel, cobalt and iron electrodes in base. J Electroanal Chem 2010;641:119-30.

[25] Hu C-C, Wu Y-R. Bipolar performance of the electroplated ironenickel deposits for water electrolysis. Mater Chem Phys 2003;82:588-96.

[26] Roy A, Watson S, Infield D. Comparison of electrical energy efficiency of atmospheric and high-pressure electrolysers. Int J Hydrogen Energy 2006;31:1964-79.